Photodegradation of gaseous volatile organic compounds (VOCs) using TiO_2 photoirradiated by an ozone-producing UV lamp: decomposition characteristics, identification of by-products and water-soluble organic intermediates

Juyoung Jeong[a], Kazuhiko Sekiguchi[a,*], Wookeun Lee[b], Kazuhiko Sakamoto[a]

[a] Department of Environmental Science and Human Engineering, Graduate School of Science and Engineering, Saitama University, 255 Shimo-ohkubo, Sakura, Saitama 338-8570, Japan
[b] Department of Environmental Engineering, Kangwon National University, Hyoja, Chuncheon, Kangwon 200-701, Korea

Abstract

The photodegradation of the toluene and benzene with TiO_2 (P25) and $UV_{254+185\,nm}$ radiation from an ozone-producing UV lamp was studied. The VOCs were decomposed and mineralized efficiently owing to the synergistic effect of photochemical oxidation in the gas phase and photocatalytic oxidation on the TiO_2 surface. The conversion levels obtained with $UV_{254+185\,nm}$ photoirradiated TiO_2 were much higher than those with conventional UV sources ($UV_{365\,nm}$ and $UV_{254\,nm}$), which suffer from both catalyst deactivation and the generation of harmful intermediates. The products from the photodegradation of VOCs with the $UV_{254+185\,nm}$ photoirradiated TiO_2 were mainly mineralized CO_2 and CO, but some water-soluble organic intermediates were also formed under more severe reaction conditions. The water-soluble aldehydes and carboxylic intermediates disappeared from the effluent gas stream and were detected in the water impingers. These findings suggest that the intermediates can be washed out by conventional gas washing technique, such as wet scrubber. Excess ozone could be easily removed by means of an MnO_2 ozone-decomposition catalyst.
© 2004 Elsevier B.V. All rights reserved.

Keywords: VOCs; Photochemical oxidation; Photocatalytic oxidation; Ozone UV lamp; Catalyst deactivation; Ozone-decomposition catalyst

1. Introduction

Volatile organic compounds (VOCs) are commonly found in the indoor air of residences and office buildings, as well as in various industrial processes, waste streams, and disposal facilities. Many VOCs can cause headaches, eye, nose, and throat irritation, and dizziness. In addition, some are suspected or known human carcinogens [1]. Traditional methods for removing VOCs from the polluted air stream, such as absorption, incineration, and condensation, have inherent limitation, such as high cost, short and unpredictable life spans, and secondary pollution.

Ultraviolet-induced oxidation techniques, including photocatalytic oxidation (PCO) and photochemical oxidation, have been extensively studied as promising methods for removing and destroying various VOCs in polluted air. PCO using titanium dioxide (TiO_2) is cost-effective and can be carried out at room temperature and atmospheric pressure, and the catalyst is stable. Despite these advantages, some critical obstacles to the further application of this technique have been reported. The generation of undesirable intermediates, some of which are more toxic than the parent compounds, is one limiting factor [2,3]. Catalyst deactivation by some pollutants, such as aromatic compounds, is also a serious problem [4–8]. In addition, the photoactivity, depends on the pollutants chemical properties and inhibitory effect of water molecules, which requires to be solved for further ap-

plications of the photocatalysis. Various approaches to overcome these drawbacks have been studied in the worldwide, for instance, the synthesis of nano-sized or visible-light TiO_2, novel metal-deposition methods, and plasma assisted photocatalysis, etc. [9–13]. Unfortunately, it is true that information for new technology to overcome simultaneously some drawbacks of conventional photocatalysis is very rare.

On the other hand, some researchers have reported that irradiation with UV light from an ozone-producing UV lamp photochemically decomposes tetrachloromethane (TCM) [14], trichloroethylene (TCE), and aromatics such as benzene and toluene [15,16] in a humid air stream. However, this photochemical oxidation method has also its own limitations. The 185 nm emission that forms hydroxyl radicals and ozone in the gas phase comprises only 5% of the total irradiated UV spectrum. The formation of toxic intermediates or products resulting from incomplete oxidation of VOCs is also a serious challenge for practical application of this method.

In this study, we describe the use of an ozone-producing UV lamp as a UV source of TiO_2. We investigated the synergistic effect of applying photocatalytic and photochemical degradation to the decomposition of VOCs. Technical parameters such as residence time, initial concentration, relative humidity, and the amounts and identities of various by-products, which must be considered in actual application of this technique, were studied in the absence and presence of TiO_2 under $UV_{254+185\,nm}$ irradiation. We also evaluated the reduction of some of the disadvantages associated with classical photocatalytic oxidation by comparing $UV_{254+185\,nm}$ with other UV sources ($UV_{365\,nm}$ and $UV_{254\,nm}$). We focused on whether PCO using $UV_{254+185\,nm}$ could efficiently decompose high concentrations of VOCs without catalyst deactivation. For post-treatment of undesirable by-products formed under severe reaction conditions, PCO may be combined with other purification. We attempted to identify the water-soluble organic intermediates to evaluate the utility of using a gas-washing technique to eliminate them. Finally, we investigated the photogeneration characteristics of ozone, and the elimination of ozone by an ozone-decomposition catalyst (ODC).

2. Material and methods

2.1. Photoreactor and UV sources

The experimental apparatus is illustrated in Fig. 1. The 0.55 l photoreactor consisted of a Pyrex glass cylinder with five inner cylinders. The three innermost cylinders were coated with the TiO_2 catalyst, and the UV lamp was located at the center of the reactor. The photoreactor was an annular design having a wire net at the inlet. Such a design will offers the stable reaction by creating a laminar flow in the reactor, although the highest conversion ratio is not shown. Irradiation was done with three UV lamps (Sankyo Denki Co. Ltd.): a black light blue lamp ($UV_{365\,nm}$) with a maximum light intensity output at 365 nm, a GL4 germicidal lamp ($UV_{254\,nm}$)

with a maximum at 254 nm, and a GLZ4 ozone producing lamp ($UV_{254+185\,nm}$) with a maximum emission at 254 nm and a minor emission (<5%) at 185 nm. The electric power consumptions of all the UV lamps were identical (4 W).

2.2. Catalyst preparation

The catalyst was Degussa P25 TiO_2 (75% anatase/25% rutile) with a Brunauer–Emmett–Teller (BET) surface area of $50\,m^2\,g^{-1}$. A sonicated mixture of 5 g of the TiO_2 in 300 ml of deionized water was dip-coated onto the innermost three cylinders of the photoreactor, and the cylinders were dried at $150\,°C$ for 2 h in an oven. The dipping procedure was repeated four times, and then the cylinders were dried at $150\,°C$ for 24 h. After the dipping procedure, the TiO_2 load on the insides of the cylinders was approximately 40 mg (ca. $0.15\,mg\,cm^{-2}$). The surface state of the coated TiO_2 and its catalytic ability were regularly checked by measuring their toluene decomposition ability at the same reaction conditions. In addition, the cylinders were newly dip-coated with TiO_2 with the same coating procedure every 6 months.

The ozone-decomposition catalyst (Nippon Syokubai Co. Ltd.) was a honeycomb type consisting of an MnO_2 active element on a TiO_2/SiO_2 support.

2.3. Experimental procedures and methods

Gaseous toluene and benzene, the target VOCs, were fed by mixing the standard gas (VOC concentration, 405 ppmv) with high-purity clean air (N_2:O_2 = 8:2; water concentration < 20 ppmv). Water vapor was obtained by passing dried air through a porous polytetrafluoroethylene tube containing deionized water at room temperature. The reaction temperature was maintained at room temperature ($298 \pm 1\,K$). Before the gas stream containing the VOCs and water vapor was introduced into the photoreactor, humid air was passed through the illuminated photoreactor for several hours to pretreat the catalyst. The UV irradiation experiments were started after the inlet and outlet toluene concentrations were equal (1 h). The conversion of VOCs and yields of decomposition products were calculated from the following equations:

$$\text{Conversion of VOC (\%)} = \frac{[\text{VOC}]_{inlet} - [\text{VOC}]_{outlet}}{[\text{VOC}]_{inlet}} \times 100$$

Decomposition product yield (%)

$$= \frac{[\text{decomposition product}]_{produced} \times \text{product carbon number}}{[\text{VOC}]_{converted} \times \text{VOC carbon number}} \times 100$$

Meanwhile, in this study, a mineralization ratio is defined as the sum of product yield of inorganic CO_2 and CO.

2,4-Dinitrophenylhydrazine (DNPH)-silica cartridges (Waters Co. Ltd.) were used to sample aldehyde compounds in the gas stream. The sample volume was 40 l at an air-flow rate of 0.5–$0.6\,l\,min^{-1}$. The amounts of water-soluble
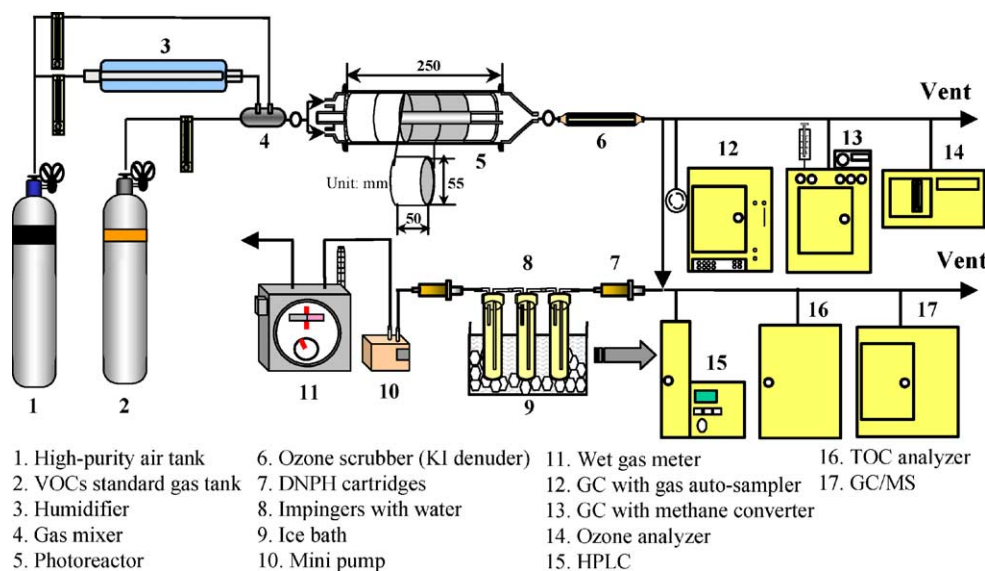
Fig. 1. Schematic diagram of the experimental apparatus.

organic intermediates were determined from the sum of total organic carbon (TOC) collected after the effluent gas was passed through a series of three impingers containing pure water. The air-flow rate ranged from 0.4 to 0.5 l min^{-1} for the sample, and the total sampled gas volume was 100 l. The water impingers were immersed in an ice/water bath to improve collection during sampling.

The impinger water was analyzed in detail to identify the various water-soluble organic intermediates collected in the water. First, the aldehydes were converted to stable hydrazone derivatives with a DNPH solution (1:1 molar ratio). After the derivatization reaction had proceeded for 12 h, the derivatized aldehydes were analyzed. Second, various carboxylic acid intermediates were identified by gas chromatography–mass spectrometry (GC–MS) employing a BF$_3$/n-butanol derivatization technique. Water samples (20 ml) were concentrated on a rotary evaporator under a vacuum to ca. 0.5 ml and then almost completely dried in a nitrogen stream. A 14% BF$_3$/butanol (0.3 ml) mixture was added to the samples, and the sample and the reagent were allowed to react at 100 °C for 30 min. Pure water (3 ml) and acetonitrile (0.3 ml) were added, and the reaction products were extracted with 5 ml of hexane. The hexane layer was washed with pure water (6 ml) and concentrated to 50 μl [18]. Meanwhile, the reactor containing an MnO$_2$ ozone-decomposition catalyst with the volume of 71.2 cm^3 was set up behind the photoreactor.

2.4. Analytical methods

The VOCs concentration was continuously monitored with a gas chromatograph (GC 14B, Shimadzu Co. Ltd.) equipped with an auto-gassampler and a flame ionization detector (FID). CO$_2$ and CO in the effluent gas were analyzed with a gas chromatograph (GC 15A, Shimadzu Co. Ltd.) equipped with a methane converter (MT-221, GL Sci-

ence Co. Ltd.) and a flame ionization detector. Aldehydes collected with both the cartridge and pure water were analyzed by a high-performance liquid chromatography (LC-9A, Shimadzu Co. Ltd.). A TOC analyzer (TOC 5000, Shimadzu Co. Ltd.) was used to quantify water-soluble organic intermediates collected in the water. The carboxylic acid derivatives were analyzed by a gas chromatography (GC 17A, Shimadzu Co. Ltd.) and a mass spectrometry (GCMS-QP5050, Shimadzu Co. Ltd.). An ozone analyzer (UVAD-1000, Shimadzu Co. Ltd.) was used to continuously monitor the gaseous ozone. In the UV$_{254+185\,nm}$ irradiation experiments, all gaseous ozone in the effluent gas was removed selectively with a potassium iodide (KI)-coated annular denuder, since ozone cannot only seriously damage the GC column [19] but also cause experimental error owing to its powerful oxidative effect on most organic compounds.

3. Results and discussion

3.1. Photodegradation of toluene with and without TiO$_2$ under UV$_{254+185\,nm}$ irradiation

3.1.1. Effect of relative humidity

The effect of relative humidity on the conversion of toluene with and without TiO$_2$ under UV$_{254+185\,nm}$ irradiation is illustrated in Fig. 2. Regardless of whether TiO$_2$ was present, the conversion of toluene increased with increasing relative humidity, reaching a peak at 40–50% humidity and then remaining constant from 40–50% to 80–90%. At all relative humidity levels, the conversion was higher in the presence of TiO$_2$ than in its absence.

When dry air is irradiated with UV$_{254+185\,nm}$, reactive oxygen species including O$_3$ and O(^{1}D) are formed via the gas-phase reactions in Eqs. (1)–(4). Moreover, in humid air,
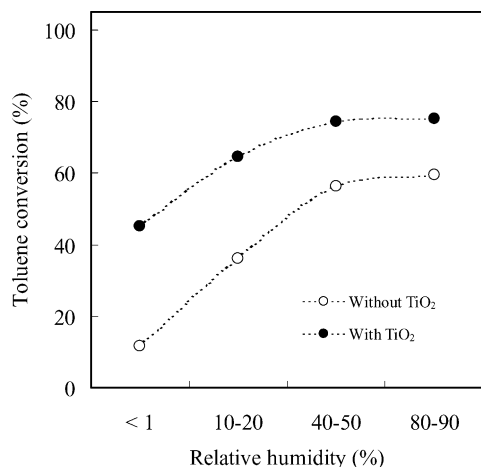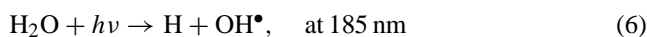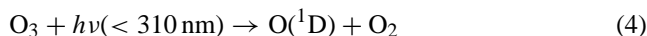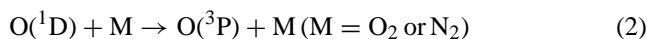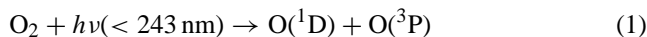
Fig. 2. The effect of relative humidity on toluene conversion with and without TiO$_2$ under UV$_{254+185\,nm}$ irradiation. [C$_7$H$_8$]$_0$, 10 ppmv; residence time, 16.5 s.

a large number of hydroxyl radicals are also formed (Eqs. (5) and (6)) [14–16,20]. Thus, photochemical oxidation of organic compounds in the gas phase is available owing to the strong oxidative effect of the abundant reactive species that form. On the other hand, as TiO$_2$ absorbs UV light with energy exceeding 3.2 eV, electron–hole pairs are generated on its surface, and they initiate redox reactions that oxidize the absorbed pollutants. Photocatalytic oxidation of organic compounds by hydroxyl radicals, which arise from the oxidation of chemisorbed water or OH$^-$, is well understood [21].

$$O_2 + h\nu(< 243\,nm) \rightarrow O(^1D) + O(^3P) \qquad (1)$$

$$O(^1D) + M \rightarrow O(^3P) + M\,(M = O_2\,or\,N_2) \qquad (2)$$

$$O(^3P) + O_2 + M \rightarrow O_3 + M \qquad (3)$$

$$O_3 + h\nu(< 310\,nm) \rightarrow O(^1D) + O_2 \qquad (4)$$

$$O(^1D) + H_2O \rightarrow 2OH^\bullet \qquad (5)$$

$$H_2O + h\nu \rightarrow H + OH^\bullet, \quad at\,185\,nm \qquad (6)$$

In the absence of TiO$_2$, the lowest conversion (ca. 12%) was observed at a humidity of less than 1%, which indicates the absolute lack of hydroxyl radicals in the reactor. The slight conversion that was observed was probably due either to photooxidation by hydroxyl radicals arising from trace water or to photolysis of toluene. The conversion increased drastically with the rise in relative humidity, owing to enhanced photochemical oxidation by generation of hydroxyl radicals via Eqs. (5) and (6) in the gas phase. We attributed the constant conversion at humidity levels above 40–50% to limitations on the UV light available to form hydroxyl radicals.

In presence of TiO$_2$, significant conversion of 45% was observed even in dry air, which implies the existence of large number of active sites on the TiO$_2$ surface. We suppose that the active sites were mainly hydroxyl radicals arising from both trace water molecules and O$_3$ on the TiO$_2$ surface. Pichat

et al. [22] have pointed out the possibility that strongly oxidizing species, such as hydroxyl radicals and O(^{1}D), are generated additionally by photodecomposition of O$_3$ on the TiO$_2$ surface. They also reported that the presence of O$_3$ on the TiO$_2$ inhibits the recombination of electrons and holes (h$^+$) and thus augments the formation rate of hydroxyl radicals from basic OH surface groups.

As was the case in the absence of TiO$_2$, the conversion increased with increasing humidity and reached a plateau at humidity levels higher than 40–50%. Many researchers have reported that the conversion of some organics may be hindered at higher humidity due to competitive adsorption between the organics and water vapor on active sites [5,23,24]. It seems, however, that because the amount of TiO$_2$ used in this study was sufficient to overcome the competition effect between toluene and water vapor on the surface of TiO$_2$, no reduction of conversion was observed at high humidity. Consequently, it became clear that using TiO$_2$ under UV$_{254+185\,nm}$ irradiation significantly enhanced the conversion of toluene relative to the conversion observed with UV irradiation alone, owing to the combined effect of photochemical oxidation in the gas phase and photocatalytic oxidation on the TiO$_2$ surface.

3.1.2. Effect of flow rate

Fig. 3 shows the effects of flow rate (residence time) on the conversion of toluene in the absence and presence of TiO$_2$ under UV$_{254+185\,nm}$ irradiation. The effects were examined at initial concentrations of 0.6 and 10 ppmv, respectively. The effect of the flow rate in the absence of TiO$_2$ differed from that observed in the presence of TiO$_2$. At 0.6 ppmv and in absence of TiO$_2$, the conversion decreased gradually as flow rate was increased from 1.0 to 4.0 l min^{-1}, which corresponds to a decrease in residence time from 33.0 to 8.3 s. We attributed the gradual reduction to decreased contact time between the reactants and hydroxyl radicals in the gas phase.

In the presence of TiO$_2$, the conversion dropped as the flow rate was reduced from 1.0 to 3.0 l min^{-1}, as was observed without TiO$_2$; but the conversion did not decrease any
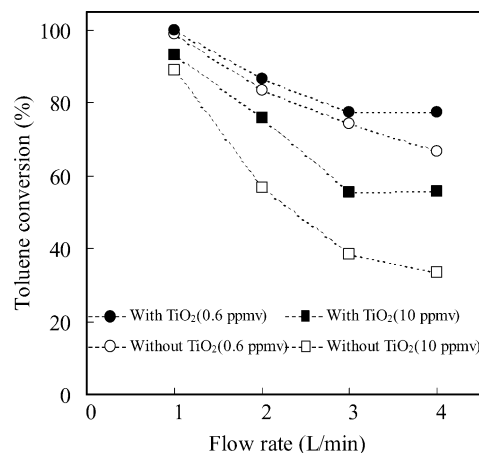

Fig. 3. The effect of flow rate on toluene conversion with and without TiO$_2$ under UV$_{254+185\,nm}$ irradiation. R.H., ca. 40–50%.

further at flow rates higher than $3 \, l \, min^{-1}$. The same behavior was also observed at an initial concentration of 10 ppmv. Alberici and Jardim [25] reported that when the flow through a photoreactor with a nonporous thin-film TiO_2 catalyst configuration can be described as laminar, the mass transfer within the reactor may be limited, and only bulk fluid-to-catalyst diffusion mass transfer will be important for the reaction of pollutants. Because our photoreactor was also designed to create a laminar flow within the reactor, bulk fluid-to-catalyst diffusion mass transfer will control the reaction between reactants and TiO_2 at low flow rates. Therefore, the gradual decrease of conversion from 1.0 to $3.0 \, l \, min^{-1}$ was probably due not only to the reduction of contact time in the gas phase but also to the limited diffusion mass transfer to the TiO_2. However, it seems that the mass transfer by turbulent flow toward the TiO_2 surface was significant at the higher flow rates ($>3 \, l \, min^{-1}$). Hence, despite the reduced contact time in the gas phase, the level of conversion could be maintained, owing to enhanced photocatalytic oxidation on TiO_2. These observations suggest that the photodegradation of VOCs can be improved by increasing the contact time between the reactants and the TiO_2, for example, by creating turbulent flow.

3.1.3. Effect of initial concentration

Fig. 4 shows the effects of initial concentration on the photodegradation of toluene in the absence and presence of TiO_2 under $UV_{254+185 \, nm}$ irradiation. High conversion was observed in the range of initial concentrations from 0.6 to 10 ppmv, regardless of the presence of TiO_2. However, in that concentration range, the mineralization behavior observed differed slightly from the conversion behavior. The mineralization decreased rapidly with the rise of initial concentration in the absence of TiO_2. In presence of TiO_2, however, a high degree of mineralization, ca. 90%, was obtained even at 10 ppmv, which confirms the photocatalytic role of the TiO_2 catalyst. Furthermore, the notable effect of TiO_2

Table 1
Conversion of toluene and benzene and yields of decomposition products with TiO_2 photoirradiated with three UV sources[a]

VOC	UV source	Conversion (%)	Product yield (%)		
			CO_2	CO	HCHO
Toluene	$UV_{365 \, nm}$	82.6	72.1	12.4	0.57
	$UV_{254 \, nm}$	83.9	73.4	14.8	0.97
	$UV_{254+185 \, nm}$	99.9	80.7	18.6	ND[b]
Benzene	$UV_{365 \, nm}$	67.1	67.7	21	0.27
	$UV_{254 \, nm}$	76.1	70.6	18.4	0.2
	$UV_{254+185 \, nm}$	94.2	78.7	16.9	ND

[a] $[C_7H_8]_0$, 0.6 ppmv; residence time, 33 s; R.H., ca. 40%.
[b] ND, below detection limit.

was clearer at 20 ppmv. These observations also suggest that $UV_{254+185 \, nm}$ can efficiently excite the TiO_2. We suppose that when the toluene-containing gas enters in the photoreactor, is initially degraded via photochemical reaction with abundant reactive species including hydroxyl radical in the gas phase, and then some of the residual organic compounds, including intermediates, transfer by spontaneous gas diffusion onto the photoirradiated TiO_2, becoming subject of the photocatalytic oxidation. As a result, through the continuous photochemical and photocatalytic processes, the toluene will be synergistically converted into nontoxic CO_2.

3.2. Comparison of different UV sources

Conversions of toluene and benzene and the yields of decomposition products obtained with TiO_2 irradiated with different UV sources are summarized in Table 1. The conversion of toluene and benzene with $UV_{254+185 \, nm}$ was much higher than that observed with $UV_{365 \, nm}$ and $UV_{254 \, nm}$. In addition, mineralization was enhanced, and the generation of harmful HCHO was inhibited significantly. When the TiO_2 catalyst was irradiated with $UV_{365 \, nm}$ or $UV_{254 \, nm}$, only photocatalytic oxidation will be of importance for the decomposition of pollutants, although photolysis of some organics is feasible under $UV_{254 \, nm}$ irradiation [26]. However, with $UV_{254+185 \, nm}$ irradiation, photochemical oxidation in the gas phase and photocatalytic oxidation on the TiO_2 surface are available simultaneously for photodegradation of VOCs, as mentioned earlier.

The effects of initial concentration on the conversion of toluene were examined with TiO_2 under three UV sources ($UV_{365 \, nm}$, $UV_{254 \, nm}$, and $UV_{254+185 \, nm}$), and the results are shown in Fig. 5. At an initial concentration of 0.6 ppmv and with $UV_{365 \, nm}$ or $UV_{254 \, nm}$ irradiation, the conversion of toluene was approximately 82% and did not drop at longer irradiation times. In contrast, at 10 ppmv, the conversion dropped drastically with increasing irradiation time. The color of the catalyst changed from white to brown. It has frequently been reported that catalyst deactivation during PCO of some aromatic compounds is attributable to irreversible deposition of less-reactive intermediates on the TiO_2 surface [5]. At 0.6 ppmv under $UV_{365 \, nm}$ or $UV_{254 \, nm}$ irradiation,
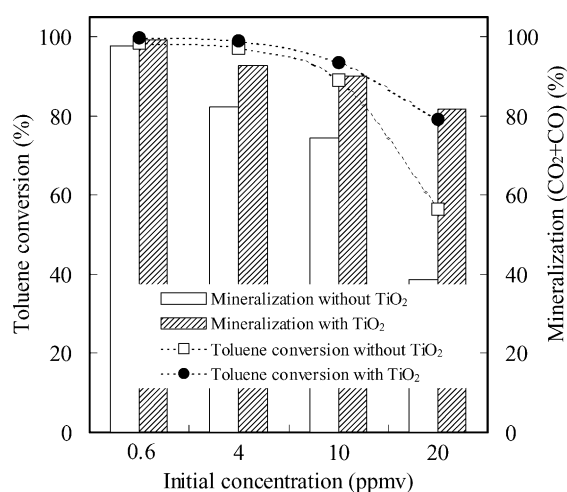

Fig. 4. The effect of initial concentration on conversion and mineralization of toluene with and without TiO_2 under $UV_{254+185 \, nm}$ irradiation. Residence time, 33 s; R.H., ca. 40–50%.
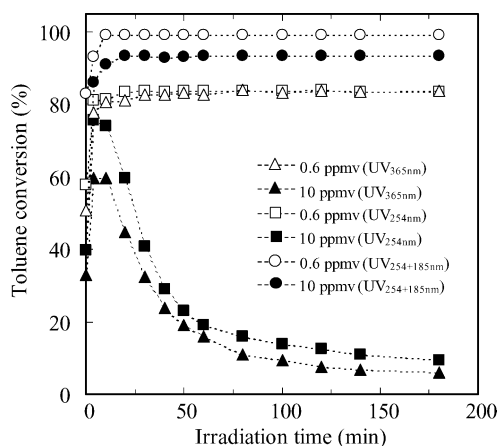
Fig. 5. The effect of initial concentration on toluene conversion with TiO_2 irradiated with three UV sources. Residence time, 33 s; R.H., ca. 40–50%.

the oxidation of the less-reactive intermediates was probably faster than deposition on the catalyst surface, owed to there being a sufficient number of active sites on the TiO_2. In contrast, the very different behavior at 10 ppmv indicates that severe catalyst deactivation must have occurred.

We found that under $UV_{254+185\,nm}$ irradiation, a high conversion ratio, greater than 95%, was achieved even at 10 ppmv, without any deactivation. The TiO_2 catalyst did not change color during PCO. We suppose that photogenerated O_3 play a key role in inhibiting catalyst deactivation by efficiently decomposing carbon deposits on the catalyst surface. The inhibitory effect of catalyst deactivation by adding the ozone into TiO_2/UV process has been previously reported [17]. These findings indicate that PCO using $UV_{254+185\,nm}$ may be effective for the treatment of gas streams containing high concentrations of VOCs. The photodegradation of VOCs, therefore, could be increased by the use of $UV_{254+185\,nm}$, which would overcome some of the crucial disadvantages associated with classical photocatalytic degradation.

Table 1 shows that the conversion of toluene was higher than that of benzene no matter what the UV source. Some studies reported that the rate of reaction of benzene, toluene, ethylbenzene, *o*-xylene (BTEX) with hydroxyl radicals decreased in the order *o*-xylene > ethylbenzene > toluene > benzene in the atmosphere. Therefore, we attributed the dif-

ference in the conversions of toluene and benzene to the difference in reaction rate with hydroxyl radicals in the gas phase and on the TiO_2 surface [16,23,27].

3.3. Identification of by-products of toluene and benzene with $UV_{254+185\,nm}$ photoirradiated TiO_2

3.3.1. Yield of decomposition products and proportion of water-soluble organic intermediates

Table 2 shows the conversion of toluene and benzene and the yields of decomposition products, including the water-soluble portion, under various reaction conditions. The use of TiO_2 under $UV_{254+185\,nm}$ irradiation (Run 2) led to an increase in mineralization to CO_2 and CO as well as in conversion, relative to that observed in the absence of TiO_2 (Run 1). The main gaseous products from toluene and benzene degradation with $UV_{254+185\,nm}$ irradiated TiO_2 were mineralized CO_2 and CO. But undesirable organic intermediates were also generated under severer reaction conditions. Almost complete conversion of toluene was achieved at the relatively low concentration of 4 ppmv (Run 3), with conversion and mineralization values of >99% and 92%, respectively. Furthermore, most of the formed organic intermediates were collected in the water impingers, which indicates their water solubility or polarity. We found that raising the initial concentration or flow rate not only reduced toluene conversion and mineralization but also increased undesirable organic intermediates (Runs 4 and 5). However, it is worthwhile to note that the water-soluble organic portion collected in the water impingers was enhanced with the increase of the undesirable organic intermediates. The collecting effects of the water were also observed in the photodegradation of benzene (Run 6).

We made an effort to quantify the collection of organic intermediates by the water impingers. We measured the aldehydes in the gas stream before and after it passed through the water impingers, and we qualitatively and quantitatively evaluated the organic intermediates collected in the water by means of high-performance liquid chromatography and GC–MS. The results of these experiments are summarized in Table 3 and Fig. 6. After the effluent gas was passed through the water impingers, no aldehydes were detected in the effluent gas stream, which implies that most of them were collected in the water. This tendency was observed regardless of

Table 2
Conversion of toluene and benzene and yields of decomposition products in some reaction conditions with and without TiO_2 under $UV_{254+185\,nm}$ irradiation[a]

Run number	VOC	TiO_2	Concentration, residence time	Conversion (%)	Product yield (%)		
					CO_2	CO	WSOC[b]
Run 1	C_7H_8	Without	10 ppmv, 33 s	89.1	48.9	24.5	10.6
Run 2	C_7H_8	With	10 ppmv, 33 s	93.5	74.1	16.1	6.0
Run 3	C_7H_8	With	4 ppmv, 33 s	99.0	75.5	17.1	8.5
Run 4	C_7H_8	With	20 ppmv, 33 s	79.1	69.3	12.6	12.8
Run 5	C_7H_8	With	10 ppmv, 16.5 s	79.9	62.4	13.5	19.3
Run 6	C_6H_6	With	10 ppmv, 33 s	92.1	78.6	11.6	13.4

[a] R.H., ca. 40–50%.
[b] WSOC, water-soluble organic compounds.

Table 3
Aldehyde concentrations in effluent gas stream before and after passing through the water impingers and in the collecting water[a]

Aldehydes detected	Before water impinger (ppbv)	After water impinger (ppbv)	In the water (ppbv)
Without TiO_2			
Formaldehyde	100.0 (±10.0)	ND[b]	118.8 (±5.8)
Acetaldehyde	113.7 (±4.1)	8 (±2.1)	80.9 (±14.0)
Benzaldehyde	Trace[c]	ND	Trace
With TiO_2			
Formaldehyde	295.0 (±8.0)	ND	331.5 (±24.5)
Acetaldehyde	56.9 (±5.2)	ND	23.9 (±8.5)
Benzaldehyde	Trace	ND	Trace

[a] $[C_7H_8]_0$, 20 ppmv; R.H., 40–50%; residence time, 33 s; collection velocity, 0.4–0.5 l min^{-1}; total collection volume, 100 l.
[b] ND, below detection limit.
[c] Trace, below quantification limit.

whether TiO_2 was present. Furthermore, most of the disappeared aldehydes in the effluent gas stream were detected in the collecting water. Fig. 6 shows the chromatograms of the various water-soluble organic compounds detected in the collecting water by GC–MS without and with TiO_2 catalyst. The detected compounds included oxalic acid, malonic acid, succinic acid, pyruvic acid, glyoxylic acid, methylglyoxal, and 4-oxobutanoic acid, maleic acid, which are commonly found in the atmosphere [18]. Some compounds disappeared or exhibited reduced peak intensity when TiO_2 was used. These results indicate that the formed organic intermediates may be washed out by conventional gas-washing methods such as a wet scrubber. On the basis of these results, therefore, we propose that the combination of PCO using UV$_{254+185\,nm}$ and a gas-washing technique has considerable potential as an effective method for the purification of refractory VOCs.

On the other hand, the fact that the CO generation rate exceeded ca. 10% under all the tested reaction conditions is problematic. The CO generation rate observed at low VOC levels was negligible, but it may be serious at high VOC levels, since CO is also a toxic indoor air pollutant. Driessen

et al. [28] reported that CO is often one of the main by-products in many PCO processes of VOCs and that it is not easily eliminated by PCO, owing to its chemical stability. It is noteworthy that the oxidation of CO to CO_2 was promoted by the use of TiO_2, because the photooxidation may be enhanced considerably by increasing the contact time of the reactants and the TiO_2 surface. In addition, platinized TiO_2 is also available, which shows a high oxidation rate on CO [29].

3.3.2. Ozone formation and elimination

Fig. 7 shows the ozone-generation characteristics under some reaction conditions with UV$_{254+185\,nm}$ irradiation and the effect of an ODC. The highest ozone concentration, ca. 140 ppmv, was recorded in dry air without TiO_2. We found that the addition of water vapor and TiO_2 reduced the ozone generation in the reactor. In the reactions without TiO_2, most of 185 nm radiation emitted from the ozone-producing UV lamp appeared to be spent on reaction with molecular oxygen (Eq. (1)), which allowed significant amounts of gaseous ozone to form in the gas phase. However, the formation of ozone was probably inhibited in humid air, due to competi-
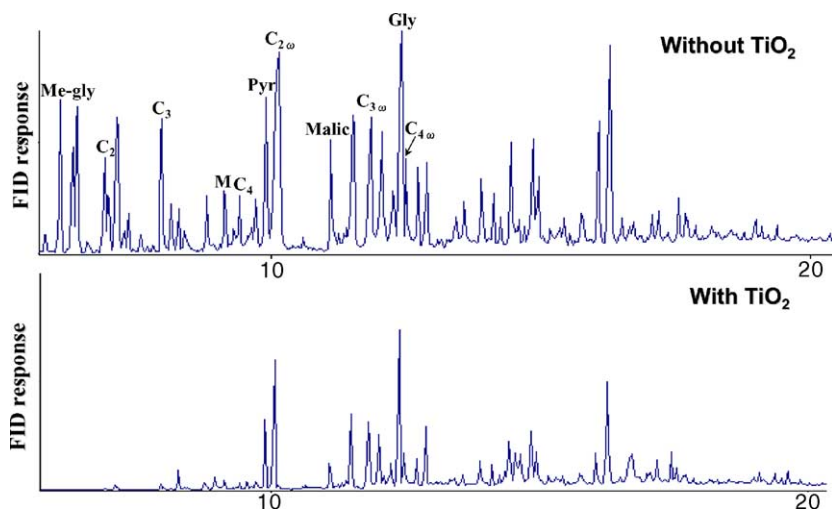

Fig. 6. Total ion chromatogram of water-soluble organic compounds detected in the collecting water by GC–MS using a BF$_3$/n-butanol derivatization technique. $[C_7H_8]_0$, 20 ppmv; residence time, 33 s; R.H., ca. 40–50%. Abbreviations: C_2, oxalic acid; C_3, malonic acid; C_4, succinic acid; $C_2\omega$, 2-oxoethanoic (glyoxylic acid); $C_3\omega$, 3-oxopropanoic acid; $C_4\omega$, 4-oxobutanoic acid; Me-Gly, methylglyoxal; M, maleic acid; Pyr, pyruvic acid; Gly, glyoxal.
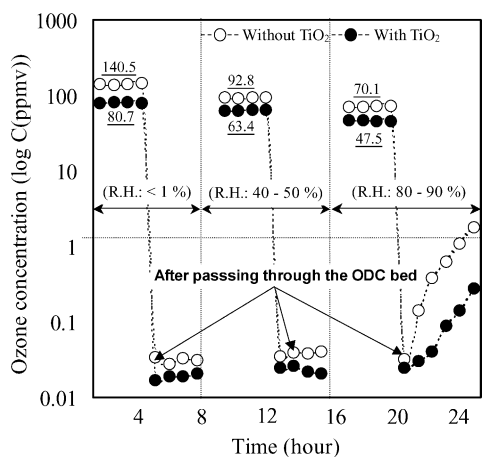
Fig. 7. Ozone-generation characteristics with $UV_{254+185\,nm}$ irradiation and ozone elimination with an MnO_2 ODC. Residence time at photoreactor, 33 s; space velocity at ODC bed, 842 h^{-1}.

tive absorption of the 185 nm radiation by ozone and water molecules. This suggestion was confirmed by the greater reduction in ozone concentration at higher relative humidity. Pichat et al. [22] reported that since the electron affinity of ozone is 2.1 eV and that of O_2 is 0.44 eV, ozone can more easily capture the photogenerated electrons on TiO_2, forming unstable oxygen species such as $O(^1D)$ or O_3^-. Hence, the remarkable reduction of ozone in the presence of TiO_2 was probably due to reductive degradation of the ozone on the TiO_2 surface.

The photogenerated excess ozone was degraded using an MnO_2 ODC bed set up downstream the photoreactor. The ODC exhibited dramatic catalytic activity for the decomposition of surplus ozone, although the activity depended on relative humidity. Ozone concentrations of 140–65 ppmv at humidity levels less than 40–50% were decomposed dramatically to World Health Organization-recommended ozone limits in air. We found, however, that humidity levels above 80% rapidly deactivated the ODC. Ozone in the effluent gas began to increase with time, which implies the breakdown of ozone-decomposition ability. We attributed the deactivation to competition between water molecules and ozone for adsorption on active sites over the catalyst. These findings suggest that dehumidification of effluent gas from photoreactor is necessary for complete decomposition of the excess ozone.

4. Conclusions

The use of TiO_2 with $UV_{254+185\,nm}$ irradiation significantly enhanced the photodegradation of VOCs relative to UV alone, owing to the combined effect of photochemical degradation in the gas phase and photocatalytic degradation on TiO_2. We suppose that when the toluene-containing gas enters in the photoreactor, is initially degraded via photochemical reaction with abundant reactive species including hydroxyl radical in the gas phase, and then some of the resid-

ual organic compounds, including intermediates, transfer by spontaneous gas diffusion onto the photoirradiated TiO_2, becoming subject of the photocatalyitc oxidation. Furthermore, the conversion of VOCs by $UV_{254+185\,nm}$ photoirradiated TiO_2 was much higher than that obtained by irradiation with conventional UV sources ($UV_{365\,nm}$ and $UV_{254\,nm}$), and the former showed improvement in some of the crucial disadvantages associated with classical photocatalytic degradation. In particular, the inhibition of catalyst deactivation may permit the application of this technique to the treatment of gas streams containing high concentrations of VOCs. The main gaseous products obtained from VOCs with the $UV_{254+185\,nm}$ irradiated TiO_2 were mineralized CO_2 and CO, but undesirable organic intermediates were also generated under more severe reaction conditions. However, these intermediates could easily be trapped by water, owing to their water solubility. Water-soluble aldehydes and carboxylic acid intermediates disappeared from the effluent gas stream and were detected in the collection water. This finding indicates that a gas-washing technique may be useful as post-treatment of organic intermediates from VOCs photodegradation. Under $UV_{254+185\,nm}$ irradiation, both ozone production and its decomposition by an ODC were dependent on the relative humidity in the gas stream, which suggests that dehumidification before the ODC bed is necessary for high levels of ozone decomposition.

References

[1] H.T.Th. Bloemen, J. Burn, Chemistry and Analysis of Volatile Organic Compounds in the Environment, first ed., Blackie Academic & Professional, London/Tokyo, 1993.
[2] M.B. Ray, Dev. Chem. Eng. Miner. Process. 8 (5/6) (2000) 405–439.
[3] W. Wang, Y. Ku, J. Photochem. Photobiol. A: Chem. 159 (2003) 47–59.
[4] M.M. Ameen, G.B. Raupp, J. Catal. 184 (1999) 112–122.
[5] L. Cao, Z. Gao, S.L. Suib, T.N. Obee, S.O. Hay, J.D. Freihaut, J. Catal. 196 (2000) 253–261.
[6] M.C. Blount, J.L. Falconer, Appl. Catal. B: Environ. 39 (2002) 39–50.
[7] H. Einaga, S. Futamura, T. Ibusuki, Appl. Catal. B: Environ. 38 (2002) 215–225.
[8] G. Martra, S. Coluccia, L. Marchese, V. Augugliaro, V. Loddo, L. Palmisano, M. Schiavello, Catal. Today 53 (1999) 695–702.
[9] A.J. Maira, K.L. Yeung, J. Soria, J.M. Coronado, C. Belver, C.Y. Lee, V. Augugliaro, Appl. Catal. B: Environ. 29 (2001) 327–336.
[10] X.Z. Li, F.B. Li, C.L. Yang, W.K. Ge, J. Photochem. Photobiol. A: Chem. 141 (2/3) (2001) 209–217.
[11] H. Ichiura, T. Kitaoka, H. Tanaka, Chemosphere 51 (2003) 855–860.
[12] D.S. Muggli, L. Ding, Appl. Catal. B: Environ. 32 (2001) 181–194.

[13] M.S. Kang, B.J. Kim, S.M. Cho, C.H. Chung, B.W. Kim, G.Y. Han, K.J. Yoon, J. Mol. Catal. A: Chem. 180 (2002) 125–132.

[14] J.H. Wang, M.B. Ray, Sep. Purif. Technol. 19 (2000) 11–20.

[15] C. Feiyan, S.O. Pehkonen, M.B. Ray, Water Res. 36 (2002) 4203–4214.

[16] H. Kohno, M. Tamura, K. Sakamoto, J. Jpn. Air Clean. Assoc. 34 (4) (1996) 37–44 (in Japanese).

[17] Z. Pengyi, L. Fuyan, Y. Gang, C. Qing, Z. Wanpeng, J. Photochem. Photobiol. A: Chem. 156 (2003) 189–194.

[18] K. Kawamura, Anal. Chem. 65 (1993) 3505–3511.

[19] E.L. Williams II, D. Grosjean, Environ. Sci. Technol. 24 (1990) 811–814.

[20] K. Sekiguchi, O. Ishitani, K. Sakamoto, in: Proceedings of the 8th International Conference on Indoor Air Quality Climate, Edinburgh, Scotland, 1999, pp. 695–700.

[21] J. Zhao, X. Yang, Build. Environ. 38 (2003) 645–654.

[22] P. Pichat, J. Disdier, C. Hoang-van, D. Mas, G. Goutailler, C. Gaysee, Catal. Today 63 (2000) 363–369.

[23] C.H. Ao, S.C. Lee, C.L. Mak, L.Y. Chan, Appl. Catal. B: Environ. 42 (2002) 119–129.

[24] T.N. Obee, S.O. Hay, Environ. Sci. Technol. 31 (2002) 2034–2038.

[25] R.M. Alberici, W.F. Jardim, Appl. Catal. B: Environ. 14 (1997) 55–68.

[26] C.C. Wong, W. Chu, Chemosphere 50 (2003) 981–987.

[27] J.G. Calvert, R. Atkinson, K.H. Becker, R.M. Kamens, J.H. Seinfeld, T.J. Wallington, G. Yarwood, The Mechanisms of Atmospheric Oxidation of Aromatic Hydrocarbons, Oxford University Press, Oxford, 2002.

[28] M.D. Driessen, A.L. Goodman, T.M. Miller, G.A. Zaharias, V.H. Grassian, J. Phys. Chem. B 102 (1998) 549.

[29] S.M. Hwang, M.C. Lee, W. Choi, Appl. Catal. B: Environ. 46 (2003) 49–63.